Immune Response Model Fitting to CD4$^+$ T Cell Data in *Lymphocytic Choriomeningitis Virus* LCMV infection

Atefeh Afsar, Filipe Martins, Bruno M. P. M. Oliveira, and Alberto A. Pinto

Abstract We make two fits of an ODE system with 5 equations that model immune response by CD4$^+$ T cells with the presence of regulatory T cells (Tregs). We fit the simulations to data regarding gp61 and NP309 epitopes from mice infected with *lymphocytic choriomeningitis virus* LCMV. We optimized parameters relating to: the T cell maximum growth rate; the T cell capacity; the T cell homeostatic level; and the ending time of the immune activation phase after infection. We quantitatively and qualitatively compare the obtained results with previous fits in the literature using different ODE models and we show that we are able to calibrate the model and obtain good fits describing the data.

Keywords T cells · Regulatory T cells (Tregs) · *Lymphocytic choriomeningitis virus* (LCMV) · Epitope gp61 · Epitope NP309 · Antigenic stimulation · Residuals · Fits

1 Introduction

The immune system has many components, one of the most important being T cells, a type of lymphocyte that develops in the thymus. The invasion by a pathogen will result in Antigen presenting cells (APC) [3] presenting the pathogen's characteristic peptides. T cells are activated by their specific antigen and start secreting cytokines, e.g. interleukine 2 (IL-2), in order to alert other cells of the immune system and to promote proliferation [29]. Occasionally, a mistake may happen and a clonotype of

A. Afsar · F. Martins (✉) · A. A. Pinto
LIAAD–INESC TEC, Department of Mathematics, Universidade do Porto, Rua do Campo Alegre, 687, 4169-007 Porto, Portugal
e-mail: luis.f.martins@inesctec.pt

A. A. Pinto
e-mail: aapinto@fc.up.pt

B. M. P. M. Oliveira
LIAAD–INESC TEC, Faculdade de Ciências da Nutrição e Alimentação da Universidade do Porto, Rua do Campo Alegre, 823, 4150-180 Porto, Portugal
e-mail: bmpmo@fcna.up.pt

A. Pinto and D. Zilberman (eds.), *Modeling, Dynamics, Optimization and Bioeconomics IV*, Springer Proceedings in Mathematics & Statistics 365,
https://doi.org/10.1007/978-3-030-78163-7_1

T cells is stimulated by self-antigens, resulting in an auto-immune response. The role of Regulatory T cells (Tregs), a subset of T cells, is to prevent such auto-immunity through their immune suppressive action. In particular, Tregs inhibit cytokine secretion by T cells [6, 25, 26]. Mis-regulation of Tregs may result in the appearance of auto-immune diseases such as IPEX [24].

There has been as increasing interest in mathematical modelling of immune responses based on both in vivo or in vitro data. See the reviews by Zhu et al. [29, 30]. There are several mathematical modelling techniques that have been used to model immune responses by T cells. See Callard et al. [11] and Lythe et al. [18] for reviews. León et al. [16] used a hypergeometric distribution in a discrete model, while de Boer et al. [12], Burroughs et al. [6], Pinto et al. [23], Blyuss et al. [4] and Khailaie et al. [15] studied systems of ordinary differential equations (ODE). In this work we will use the ODE model in Pinto et al. [23] developed from the article from Burroughs et al. [6]. A 7 ODE model with two T cell clonotypes was used in Atefeh et al. [1] to fit the time dynamics data from Homann et al. [14].

Here, we aim to use the model with 5 ODE from Pinto et al. [23], that will allow us to make two separate fits to the data from Homann et al. [14], one fit for epitope gp61 and another fit for epitope NP309. In Sect. 2, we present the immune response model. Afterwards, in Sect. 3, we fit the model to the data. We discuss and analyse the fits in Sect. 4 and we finish with some conclusions in Sect. 5.

2 Immune Response Model

We consider the set of 5 ordinary differential equations from Sect. 3 in Pinto et al. [23] to model $CD4^+$ T cells and regulatory T cells. Tregs are activated at a rate a by self antigens from an inactive state denoted by R, to an active state denoted by R^*. Similarly, T cells are activated at a rate b by their specific antigen to the IL-2 secreting state T^* from the non-secreting state T. All cells proliferate when they adsorb IL-2 cytokines. We also consider an inflow of immune T cells into the tissue (T_{in}) and Tregs (R_{in}), which can represent T cell circulation or naïve T cells from the thymus.

The model consists of a set of five ordinary differential equations. We have an equation for each T cell population (inactive Tregs R, active Tregs R^*, non-secreting T cells T, secreting or activated T cells T^*) and interleukine 2 density I.

$$
\begin{aligned}
\frac{dR}{dt} &= (\varepsilon\rho I - \beta(R + R^* + T + T^*) - d_R)R + \hat{k}(R^* - aR) + R_{in},\\
\frac{dR^*}{dt} &= (\varepsilon\rho I - \beta(R + R^* + T + T^*) - d_{R^*})R^* - \hat{k}(R^* - aR),\\
\frac{dT}{dt} &= (\rho I - \beta(R + R^* + T + T^*) - d_T)T + k(T^* - bT + \gamma R^* T^*) + T_{in},\\
\frac{dT^*}{dt} &= (\rho I - \beta(R + R^* + T + T^*) - d_{T^*})T^* - k(T^* - bT + \gamma R^* T^*),
\end{aligned}
$$

$$\frac{dI}{dt} = \sigma(T^* - (\alpha(R + R^* + T + T^*) + \delta)I).$$

The parameter values used and obtained in the fits are presented in the Appendix, in Tables 1 and 2. As in Afsar et al. [1], we will consider death rates to be equal $d_T = d_R$ and $d_{R^*} = d_{T^*}$, and also equal relaxation rates $k = \hat{k}$. The inflow of T cells T_{in} can be different from the inflow of Tregs R_{in}. Further details of the model are presented in Burroughs et al. [5–10], Oliveira et al. [21, 22], Pinto et al. [23] and Yusuf et al. [28].

3 Simulations and Fits

In this section we describe our methods and do the fits of the model to two time series of the immune response by CD4$^+$ T cells to *lymphocytic choriomeningitis virus* - LCMV in mice obtained from laboratory experiments from Homann et al. [14]. Each of the time series that constitute the data regarding the concentration of T cells that responded to each of the two different LCMV epitopes studied, the gp61 (14 data points) and the NP309 (8 data points).

Previously published articles provided the estimates for most of the parameter values [2, 6, 20, 21, 27] and we considered that the parameters in Table 1 are fixed. The parameters to be fitted are in Table 2. Their admissible range was obtained from the literature [6, 19, 21]. These parameters are: the T cell maximum growth rate ρ/α; the T cell capacity $T^{cap} = \rho/(\alpha\beta)$; the homeostatic T cell level T^{hom} which is related to the T cell inflow T_{in} by $T_{in} \approx T^{hom} d_T$, assuming no antigenic stimulation of T cells $b = 0$ and small homeostatic values $T^{hom} + R^{hom} << T^{cap}$. See [23] for further details. Note that the parameters used in the optimization procedure are related to the T cells activated by their respective epitope, while the parameters related with Tregs and the parameters related with cytokines were fixed.

Following Afsar et al. [1], we assumed that the T cells were stimulated by the pathogen between the inoculation time $t = 0$ and a final time t_{end}. Hence, we considered a specific step function of time for the antigen simulation parameter b: a high value of the antigenic stimulation of T cells $b = 1000$ for times within $[0, t_{end}]$, and a very small value, $b = 10^{-5}$, outside that interval, see Table 1. The ending times t_{end} of high antigen stimulation intensity b corresponding to the exposition to a pathogen were also considered in the optimization procedure to fit the model to the data. See Table 2 for the fits for epitopes gp61 and NP309.

The initial condition (at time $t = 0$) corresponds to the homeostatic controlled state, with a low concentration of T cells. This state was achieved by numerically integrating the model for a long time, for a small value of antigenic stimulation of T cells, $b = 10^{-5}$.

Our objective was to minimize the sum of squares of the residuals in a logarithmic scale:

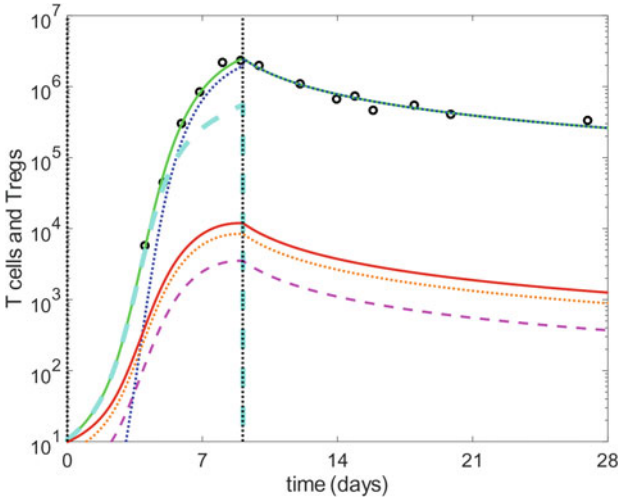

Fig. 1 Fit of the ODE model to the laboratory measurements of the CD4$^+$ T cells concentration for the gp61 epitope. The vertical axis has logarithmic scale. Green line: $T + T^*$; Blue dots: T; Cyan dashes: T^*; Red line: $R + R^*$; Orange dots: R; Violet dashes: R^*. The vertical dashed line marks the ending time $t_{end} = 9.102$ of the immune response phase. $res^2_{gp61} = 0.294$ and $MNSQ_{gp61} = 0.0294$. The parameters are shown in Tables 1 and 2

$$res^2 = \sum_{i=1}^{\#\text{data points}} \left(\log x(t_i) - \log(T(t_i) + T(t_i)^*)\right)^2$$

where #data points is the number of data points, $x(t_i)$ are the concentrations of T cells from Homann et al. [14] and t_i are the observation times, and $T(t_i) + T(t_i)^*$ represents the total T cell concentration from the fit at time t_i. The observation times range from 0 to 28 days after infection. Starting from several initial random parameter estimates, we used an iterative procedure to obtain the optimized values of the parameters. The optimized parameters for the best fit are presented in Table 2 of the appendix. The fit to the data is presented graphically in Figs. 1 and 2.

The software used for the simulations of the model was GNU Octave—*version 5.2.0*. The routine used for the numerical integration of the ODE system was `lsode`. The routine used for the optimization procedure of minimizing the residuals was `fminsearch` implementing the Nelder-Mead algorithm/downhill simplex method.

Starting from time $t = 0$ we observe in Figs. 1 and 2 that the concentration of T cells grows in a non-linear fashion, initially with the majority of T cells being secreting T cells T^*. Hence, as the IL-2 cytokine is being increasingly secreted (data not shown), we observe an increase in the growth rate of both T cells and Tregs. However, with higher concentration of Tregs, in particular, active Tregs R^*, there is an augmented relaxation rate of secreting T cells T^* to the non-secreting state T. At some point in time, around day 5 for epitope gp61 and near day 9 for epitope NP309, the concentration of secreting T cells is close to the concentration of non-secreting

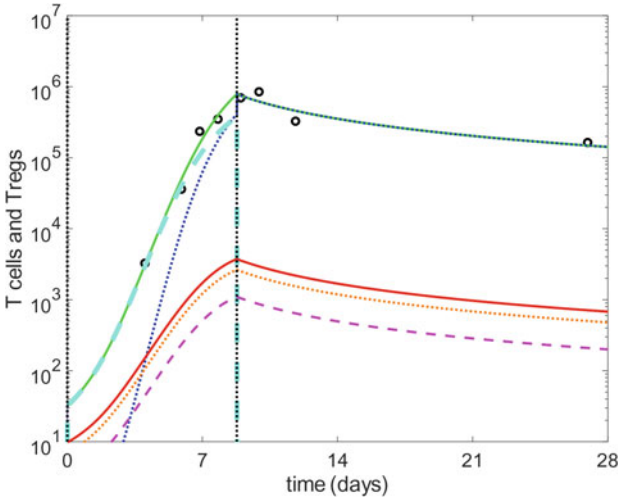

Fig. 2 Fit of the ODE model to the laboratory measurements of the CD4$^+$ T cells concentration for the NP309 epitope. The vertical axis has logarithmic scale. Green line: $T + T^*$; Blue dots: T; Cyan dashes: T^*; Red line: $R + R^*$; Orange dots: R; Violet dashes: R^*. The vertical dashed line marks the ending time $t_{end} = 8.782$ of the immune response phase. $res^2_{NP309} = 0.507$ and $MNSQ_{NP309} = 0.127$. The parameters are shown in Tables 1 and 2

T cells. After that point in time, the growth rate of T cells slows down until the end of the immune response phase. In the relaxation phase, we observe a reduction both in the concentration of T cells and Tregs due to the quick decrease of secreting T cells, and consequently the drop of IL-2 to negligible levels (data not shown), thereby stopping growth. Immediately after the end of the immune response phase, the decay in the concentrations of all cells is faster due to the action of the Fas-FasL death by apoptosis, modelled by the quadratic term with β (see more details in Afsar et al. [1] and Pinto et al. [23]). As the concentration of T cells becomes smaller, this term will have a reduced relevance in the decay and the linear death term will have a higher relative importance. We note that the concentration of inactive Tregs is higher than the concentration of active Tregs since their activation rate is relatively small $a < 1$.

For the gp61 epitope we obtained the residual sum of squares $res^2_{gp61} = 0.294$ while for the NP309 epitope we obtained $res^2_{NP309} = 0.507$ as presented in Figs. 1 and 2, respectively. Furthermore, we also present the residual mean square $MNSQ = res^2/df$ for each fit, where the number of degrees of freedom $df =$ #data points $-$#free parameters, and #free parameters $= 4$ is the number of free parameters. So we obtained, respectively, $MNSQ_{gp61} = 0.0294$ and $MNSQ_{NP309} = 0.127$.

4 Discussion

Afsar et al. [1] have previously simultaneously fitted the time series of the immune responses for epitopes gp61 and NP309 from Homann et al. [14] to a 7-ODE model. For each series, they have obtained the sum of residuals $res^2_{gp61} = 0.565$ and $res^2_{NP309} = 0.995$, and they have obtained the residual mean square $MNSQ = 0.0975$ for the simultaneous fit. Comparatively, we now obtain lower sum of residuals for both epitopes. Our residual mean square value for the epitope gp61 fit is lower than the value for the simultaneous fit from [1] while for the epitope NP309 fit it is slightly higher. This might be explained by the fact that on the simultaneous fit we have a total of $14 + 8 = 22$ data points, while having only 8 data points for the separate NP309 fit.

The same data have been analysed by de Boer et al. [13]. They have made two fits for each epitope, with a biphasic and a monophasic contraction phase respectively. For the gp61 epitope they obtained respectively $MNSQ_{gp61} = 0.06$ and $MNSQ_{gp61} = 0.17$. For the NP309 epitope they obtained respectively $MNSQ_{NP309} = 0.10$ and $MNSQ_{NP309} = 0.12$. When comparing our fits to theirs we see that for epitope gp61 fit we obtain lower residual mean square values than both their biphasic and monophasic models. For the epitope NP309 fit we obtain a higher residual mean square value, albeit very close to their value for the monophasic model.

The equations being used here are different from de Boer et al. [13]. Similarly to Afsar et al. [1], we use the same equation. We used the same equations over time and changed only one parameter in time: the antigenic stimulation of T cells b. This parameter was either in the "on" or "off" state, which is a simplification of a biologically more complex time evolution. The ending time of the immune activation phase t_{end} is a parameter in the optimization procedure and specific to each epitope. Moreover, contrary to [1] where $t_{ini} = 3.31$, here we have set the initial time of the immune activation phase $t_{ini} = 0$, which is the time when the disease is inoculated in the mice according to the experimental description in Homann et al. [14]. Opposite to de Boer et al. [13], we observe that the immune response activation seems to end earlier for epitope NP309 than for epitope gp61 ($t_{end} = 8.782$ and $t_{end} = 9.102$, respectively), but we agree with them that the peak time is quite uncertain and would require further research with different models and/or different and more frequent data around that point.

As in Afsar et al. [1], we assumed that the initial condition is the controlled homeostatic state. Regarding the homesostatic T cells level, in [1], the T^{hom} values for each T cell clonotype are 2409 and 787.74, while here we obtained $T^{hom} = 10.94$ and $T^{hom} = 32.79$ for gp61 and NP309, respectively. While the homeostatic T cells level apparently differ by two orders of magnitude, the difference is mostly explained by these values effectively working as a parameter determining the initial condition for the ODE system. Notice that around day 3, for both epitopes, our simulations have concentrations of T cells near 1000 (see Figs. 1 and 2). With respect to the value of the maximum growth rate of T cells, it is close to the one reported by de Boer et al. [13], although the "true" growth rate in our model is time dependent (see Afsar et al. [1] for more details). We estimated a higher maximum growth rate for the gp61

epitope than for the NP309 epitope, which is also the case in de Boer et al. [13]. Using the quadratic death term β allows for a smooth transition between the rapid apoptosis phase we observe around day 9 and the slower death rate we observe later, instead of two separate phases as presented in de Boer et al. [13]. We observe that this is also indirectly present in the optimization procedure since β influences T cell capacity $T^{cap} = \rho/(\alpha\beta)$.

Although the value we selected for the death rates of T cells is low, our model does not include the differentiation into memory cells, like in Afsar et al. [1], thus we used the initial 28 days of the data from Homann et al. [14]. Another limitation is to consider that the antigenic stimulation of T cells b is a step function of time instead of a smooth function, that would require more parameters. Since we have a small number of data points, the fixed parameters have the same values for both epitopes, which can be interpreted as that both clonotypes of T cells have similar characteristics. Our model has two strengths. Firstly, it has the same equations in all phases of time, the immune activation phase and the contraction phase, and without needing to consider biphasic regimes. Secondly, in our fit the free parameters were specific to the T cells responding to each epitope.

5 Conclusions

In conclusion, our model allows to achieve a good fit to the data of the immune responses from Homann et al. [14] to the gp61 and NP309 LCMV epitopes, having most of the parameters at the values described from the literature, and optimizing a set of 4 parameters related to the maximum T cell growth rate, the T cell capacity, the T cell homeostatic level, and the ending time of the immune activation phase. We discuss and interpret the results and compare our fits with other fits using different ODE models from the literature.

As future work, we could compute confidence intervals for the parameters and check for robustness of the estimated parameters using other data sets with more observations and more frequent T cell measurements over time.

Acknowledgements The authors would like to thank the financial support by FCT–Fundação para a Ciência e a Tecnologia (Portuguese Foundation for Science and Technology) as part of project UID/EEA/50014/2019 and within project "Modelling, Dynamics and Games" with reference PTDC/MAT–APL/31753/2017. Atefeh Afsar would like to thank the financial support of FCT–Fundação para a Ciência e a Tecnologia–through a Ph.D. grant of the MAP–PDMA program with reference PD/BD/142886/2018.

Appendix

The parameters of our model and their default values as well as the fitted parameters are presented in the following two tables (Tables 1 and 2).

Table 1 Parameters values for our model of T cells and Tregs from [1, 2, 6, 13, 17, 21, 27]

Fixed parameters	Symbol	Value
T cells T, T^*		
Death rate ratio of active: inactive T cells	d_{T^*}/d_T	1
Death rate of inactive T cells (day^{-1})	d_T	10^{-3}
Secretion reversion[b] (day^{-1})	k	2.4
Antigen Stimulation of T cells	b	1000
Tregs R, R^*		
Growth rate ratio Tregs: T cells	ε	0.6
Relaxation rate (day^{-1})	$\hat{k}$	2.4
Death rate ratio of inactive Tregs: inactive T cells	d_R/d_T	1
Death rate relative ratio of Tregs: T cells	$\frac{d_{R^*}}{d_R}/\frac{d_{T^*}}{d_T}$	1
Tregs antigen stimulation level (day^{-1})	$a\hat{k}$	1
Homeostatic Treg level[c] (cells day^{-1})	R^{hom}	10
Secretion inhibition	γ	$10\ R_{hom}^{-1}$
Interleukin-2 (IL-2) Cytokine		
Max. cytokine concentration[d] (pM)	$1/\alpha$	200 pM
IL2 secretion rate (pM/day)	σ	144
Cytokine decay rate (day^{-1})	$\sigma\delta$	36

[b]This is in the absence of Tregs

[c]This is in terms of the homeostatic Treg level $R_{hom} \approx \frac{R_{in}}{d_R}\left(1 - \frac{d_R - d_{R^*}}{\hat{k}(a+1)+d_R}\right)$

[d]This is taken as 20 times the receptor affinity ($10pM$)

Table 2 Fitted parameters values for our model of T cells and Tregs, with ranges adopted from [1, 6, 13, 20, 21]

Parameter	Symbol	Range	Fitted value
gp61 epitope ($res^2 = 0.294$, $MNSQ = 0.0294$)			
T cell Maximum growth rate (day^{-1})	ρ/α	< 6	3.298
Capacity of T cells (10^7 cells)	$T^{cap} = \rho/(\alpha\beta)$	$0.3 - 3$	1.847
Homeostatic T cells level[a] (cells day^{-1})	T^{hom}	$< 10^5$	10.94
End of the immune activation phase (day)	t_{end}	$6 - 15$	9.102
NP309 epitope ($res^2_{NP309} = 0.507$, $MNSQ_{NP309} = 0.127$)			
T cell Maximum growth rate (day^{-1})	ρ/α	< 6	1.702
Capacity of T cells (10^7 cells)	$T^{cap} = \rho/(\alpha\beta)$	$0.3 - 3$	0.577
Homeostatic T cells level[a] (cells day^{-1})	T^{hom}	$< 10^5$	32.79
End of the immune activation phase (day)	t_{end}	$6 - 15$	8.782

[a]T cell inflow level is given by $T_{in} = T^{hom} d_T$

References

1. Atefeh, A., Martins, F., Oliveira, B.M.P.M., Pinto, A.: A fit of CD4$^+$ T cell immune response to an infection by lymphocytic choriomeningitis virus. Math. Biosci. Eng. **16**(6), 7009–7021 (2019)
2. Anderson, P.M., Sorenson, M.A.: Effects of route and formulation on clinical pharmacokinetics of interleukine-2. Clin. Pharmacokinet. **27**, 19–31 (1994)
3. Banchereau, J., Briere, F., Caux, C., Davoust, J., Lebecque, S., Liu, Y.-J., Pulendran, B., Palucka, K.: Immunobiology of dendritic cells. Annu. Rev. Immunol. **18**(1), 767–811 (2000)
4. Blyuss, K.B., Nicholson, L.B.: The role of tunable activation thresholds in the dynamics of autoimmunity. J. Theor. Biol. **308**, 45–55 (2012)
5. Burroughs, N.J., Ferreira, M., Martins, J., Oliveira, B.M.P.M.: Alberto A. Pinto, and N. Stollenwerk. Dynamics and biological thresholds. In: Pinto, A.A., Rand, D.A., Peixoto, M.M. (eds.) Dynamics, Games and Science I, DYNA 2008, in Honor of Maurício Peixoto and David Rand, vol. 1 of Springer Proceedings in Mathematics, pp. 183–191. Springer, Berlin Heidelberg (2011)
6. Burroughs, N.J., Oliveira, B.M.P.M., Pinto, A.A.: Regulatory T cell adjustment of quorum growth thresholds and the control of local immune responses. J. Theor. Biol. **241**, 134–141 (2006). July
7. Burroughs, N.J., Ferreira, M., Oliveira, B.M.P.M., Pinto, A.A.: Autoimmunity arising from bystander proliferation of T cells in an immune response model. Math. Comput. Model. **53**, 1389–1393 (2011)
8. Burroughs, N.J., Ferreira, M., Oliveira, B.M.P.M., Pinto, A.A.: A transcritical bifurcation in an immune response model. J. Differ. Equ. Appl. **17**(7), 1101–1106 (2011). July
9. Burroughs, N.J., Oliveira, B.M.P.M., Pinto, A.A., Ferreira, M.: Immune response dynamics. Math. Comput. Model. **53**, 1410–1419 (2011)
10. Burroughs, N.J., Oliveira, B.M.P.M., Pinto, A.A., Sequeira, H.J.T.: Sensibility of the quorum growth thresholds controlling local immune responses. Math. Comput. Model. **47**(7–8), 714–725 (2008). April
11. Callard, R.E., Yates, A.J.: Immunology and mathematics: crossing the divide. Immunology **115**, 21–33 (2005)
12. de Boer, R.J., Hogeweg, P.: Immunological discrimination between self and non-self by precursor depletion and memory accumulation. J. Theor. Biol. **124**(3), 343–369 (1987). February
13. de Boer, R.J., Homann, D., Perelson, A.S.: Different dynamics of CD4+ and CD8+ T cell responses during and after acute lymphocytic choriomeningitis virus infection. J. Immunol. **171**, 3928–3935 (2003)
14. Homann, D., Teyton, L, Oldstone, M.B.A.: Differential regulation of antiviral T-cell immunity results in stable CD8+ but declining CD4+ T-cell memory. Nat. Med. 7(8), 913–919 (2001)
15. Khailaie, S., Bahrami, F., Janahmadi, M., Milanez-Almeida, P., Huehn, J., Meyer-Hermann, M.: A mathematical model of immune activation with a unified self-nonself concept. Front. Immunol. **4**, 474 (2013). December
16. León, K., Lage, A., Carneiro, J.: Tolerance and immunity in a mathematical model of T-cell mediated suppression. J. Theor. Biol. **225**, 107–126 (2003)
17. Lowenthal, J.W., Greene, W.C.: Contrasting interleukine 2 binding properties of the alpha (p55) and beta (p70) protein subunits of the human high-affinity interleukine 2 receptor. J. Exp. Med. **166**, 1155–1069 (1987)
18. Lythe, G., Molina-París, C.: Some deterministic and stochastic mathematical models of naïve T-cell homeostasis. Immunol. Rev. **285**(1), 206–217 (2018)
19. Michie, C.A., McLean, A., Alcock, C., Beverley, P.C.L.: Life-span of human lymphocyte subsets defined by CD45 isoforms. Nature **360**, 264–265 (1992)
20. Moskophidis, D., Battegay, M., Vandenbroek, M., Laine, E., Hoffmann-Rohrer, U., Zinkernagel, R.M.: Role of virus and host variables in virus persistence or immunopathological disease caused by a non-cytolytic virus. J. Gen. Virol. **76**, 381–391 (1995)

21. Oliveira, B.M.P.M., Figueiredo, I.P., Burroughs, N.J., Pinto, A.A.: Approximate equilibria for a T cell and Treg model. Appl. Math. Inf. Sci. **9**(5), 2221–2231 (2015)
22. Oliveira, B.M.P.M., Trinchet, R., Otero-Espinar, M. V., Pinto, A., Burroughs, N.: Modelling the suppression of autoimmunity after pathogen infection. Math. Methods Appl. Sci. 41(18), 8565–8570 (2018)
23. Pinto, A.A., Burroughs, N.J., Ferreira, F., Oliveira, B.M.P.M.: Dynamics of immunological models. Acta. Biotheor. **58**, 391–404 (2010)
24. Sakaguchi, S.: Naturally arising $CD4^+$ regulatory T cells for immunological self-tolerance and negative control of immune responses. Annu. Rev. Immunol. **22**, 531–562 (2004)
25. Shevach, E.M., McHugh, R.S., Piccirillo, C.A., Thornton, A.M.: Control of T-cell activation by $CD4^+$ $CD25^+$ suppressor T cells. Immunol. Rev. **182**, 58–67 (2001)
26. Thornton, A.M., Shevach, E.M.: $CD4^+$ $CD25^+$ immunoregulatory T cells suppress polyclonal T cell activation in vitro by inhibiting interleukine 2 production. J. Exp. Med. **188**(2), 287–296 (1998)
27. Veiga-Fernandes, H., Walter, U., Bourgeois, C., McLean, A., Rocha, B.: Response of naïve and memory $CD8^+$ T cells to antigen stimulation in vivo. Nat. Immunol. **1**, 47–53 (2000)
28. Yusuf, A.A., Figueiredo, I.P., Afsar, A., Burroughs, N.J., Oliveira, B.M.P.M., Pinto, A.A.: The effect of a linear tuning between the antigenic stimulations of $CD4^+$ T cells and $CD4^+$ Tregs. Mathematics 8(2), 293. (February 2020)
29. Zhu, J., Paul, W.E.: CD4 T cells: fates, functions, and faults. Blood **112**(5), 1557–1569 (2008)
30. Zhu, J., Yamane, H., Paul, W.E.: Differentiation of effector CD4 T cell populations. Annu. Rev. Immunol. **28**(1), 445–489 (2010)